
Figures and figure supplements

Distinct release properties of glutamate/GABA co-transmission serve as a frequency-dependent filtering of supramammillary inputs

Himawari Hirai *et al.*

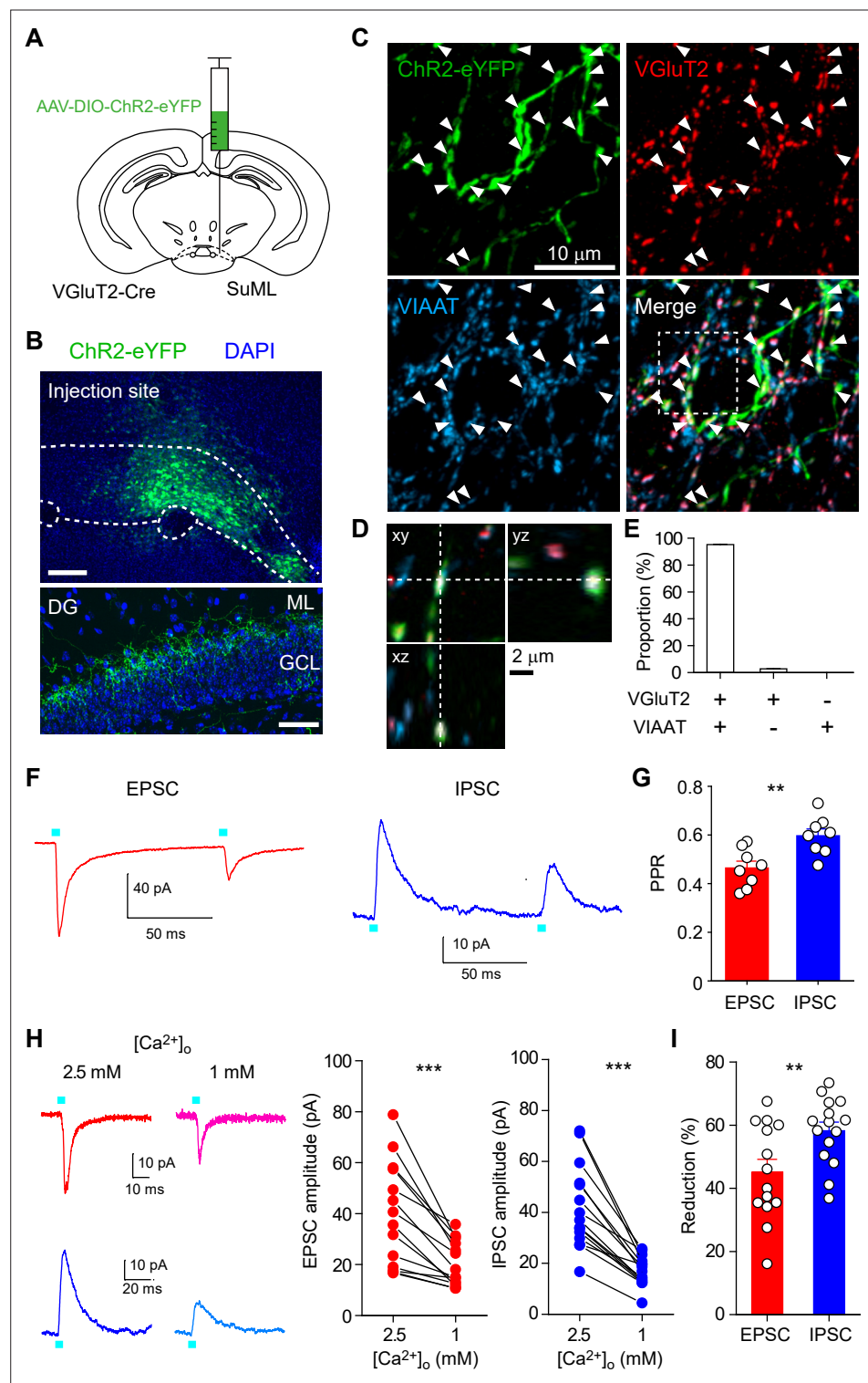


Figure 1. Different PPRs and Ca^{2+} sensitivities of glutamate/GABA co-transmission at SuM-GC synapses. (A) Diagram illustrating the injection of AAV-DIO-ChR2(H134R)-eYFP into the lateral part of SuM of VGlut2-Cre mouse. (B) (top) Fluorescence image showing the injection site of AAV in the SuM. (bottom) ChR2(H134R)-eYFP-expressing SuM axons are observed in the supragranular layer of the DG. ML, molecular layer; GCL, granule cell layer. Scale bars, Top, 200 μ m; Bottom, 50 μ m. (C) Z-stacked immunofluorescence images double stained for VGlut2 (red) and VIAAT (cyan). The merged image demonstrates the colocalization of VGlut2 and VIAAT in the ChR2-eYFP-expressing SuM terminals (arrowheads). (D) Higher magnification xy, xz, and yz projection images

Figure 1 continued on next page

Figure 1 continued

outlined in boxed area in **(C)** show that a SuM bouton is co-stained with VGluT2 and VIAAT. **(E)** Proportion of VGluT2- and/or VIAAT-expressing boutons in the ChR2-eYFP labeled boutons (2205 boutons, 7 slices). Both VGluT2 and VIAAT ($95.2 \pm 0.3\%$), VGluT2 only ($2.7 \pm 0.2\%$), and VIAAT only (0%). **(F)** Representative traces of EPSC (red, $V_h = -70$ mV) and IPSC (blue, $V_h = 0$ mV) evoked with paired pulse illumination (100 ms interval). **(G)** Summary plot of PPR showing a significant difference between EPSC and IPSC. **(H)** Representative traces (left) and summary plots (right) of EPSCs and IPSCs in 2.5 and 1 mM extracellular Ca^{2+} . **(I)** Summary plot of percent reduction in the amplitudes of EPSCs and IPSCs from 2.5 to 1 mM extracellular Ca^{2+} . Data are presented as mean \pm SEM. ** $p < 0.01$, *** $p < 0.001$.

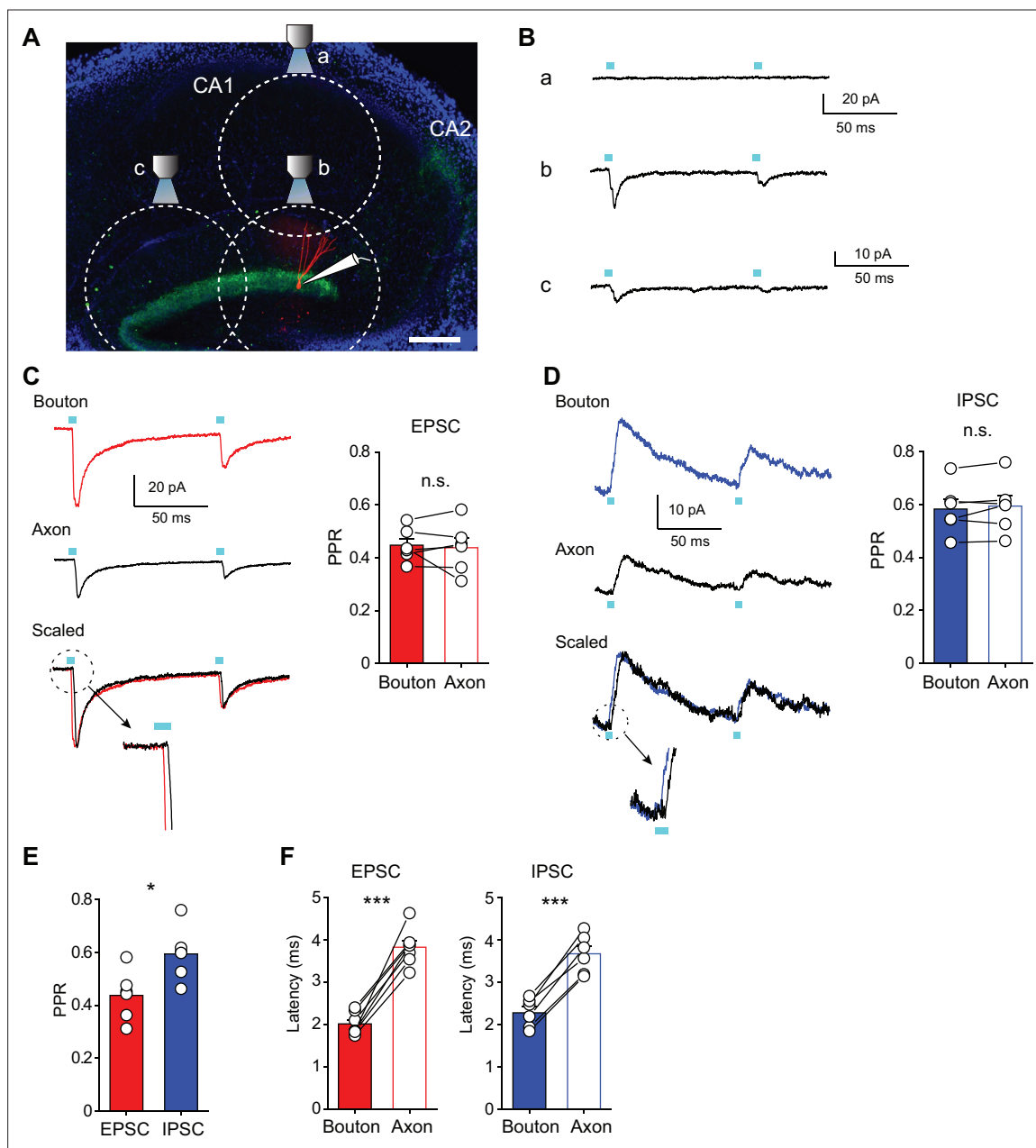


Figure 1—figure supplement 1. PPRs of glutamatergic and GABAergic co-transmission show no difference between over-axon and over-bouton illumination. **(A)** Diagram of the experimental setup. Fluorescence image of hippocampal slice shows ChR2-eYFP expressing SuM fibers (green) and a biocytin-filled GC (red). The dotted circles indicate the estimated LED illumination area at each location. We recorded from GCs located in the most edge of upper blade of GC layer (~150 μm). Once synaptic responses were observed by over-bouton illumination (over-the recorded cell soma, position b), then the objective lens was moved to ~600 μm vertically away in the stratum radiatum of the CA1 region (position a). The light power was adjusted to evoke no response at position a, indicating that SuM-GC synapses on the recorded GCs were out of the illumination field. The objective lens was then returned to position b, and PSCs of SuM-GC synapses were recorded with paired stimulation. Then, the objective lens was moved ~600 μm along the GC layer (position c) to achieve over-axon illumination. Scale bar: 200 μm. **(B)** Representative traces of SuM-GC EPSCs evoked with over-CA1 (a), over-bouton (b), and over-axon (c) illumination. **(C, D)** Representative traces (left) and summary plots of PPRs (right) of SuM-GC EPSCs (**C**) or IPSCs (**D**) indicating no significant difference between over-bouton and over-axon illumination of SuM inputs (EPSC: bouton: 0.45 ± 0.03 ; axon: 0.44 ± 0.04 , $n=6$, $p=0.72$, paired t test; IPSC: bouton: 0.58 ± 0.04 ; axon: 0.59 ± 0.04 , $n=6$, $p=0.32$, paired t test). EPSCs or IPSCs were recorded with over-bouton (top) or over-axon (middle) illumination, respectively. Bottom traces show that a trace by over-axon stimulation was scaled to the peak of a trace by over-bouton stimulation. Magnified traces of the dotted circle show a delayed onset latency of a trace by over-axon stimulation relative to a trace by over-bouton stimulation. **(E)** Summary plot of PPR indicating a significant difference between EPSC and IPSC evoked by over-axon illumination (EPSC: 0.44 ± 0.04 ; IPSC: 0.59 ± 0.04 , $n=6$, $p<0.05$, unpaired t test). **(F)** Summary plots of latency to the onset of the synaptic response. The delayed latency of

Figure 1—figure supplement 1 continued on next page

Figure 1—figure supplement 1 continued

the synaptic responses by over-axon illumination indicates that synaptic transmission was mediated by light-evoked action potential propagation toward SuM terminals (EPSC: bouton: 2.0 ± 0.1 ms; axon: 3.8 ± 0.2 ms, $n=7$, $p<0.001$, paired t test; IPSC: bouton: 2.3 ± 0.1 ms; axon: 3.7 ± 0.2 ms, $n=6$, $p<0.001$, paired t test). Data are presented as mean \pm SEM. * $p<0.05$, *** $p<0.001$, n.s., not significant.

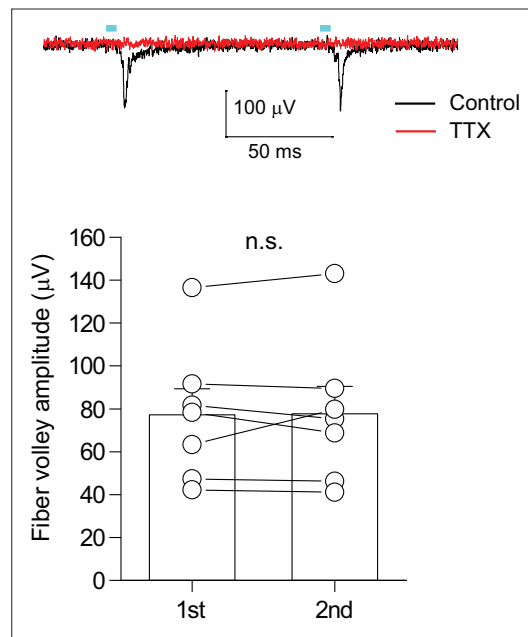


Figure 1—figure supplement 2. Paired-pulse light stimulation evoked similar amplitude of fiber volley. (top) Representative traces of the extracellularly recorded fiber volley from supragranular layer in response to paired light stimulation with 100ms interval. 1 μ M TTX completely blocked the fiber volley (red). To clearly isolate the fiber volley, light-evoked synaptic responses were blocked by 10 μ M NBQX, 50 μ M D-AP5, and 100 μ M picrotoxin. (bottom) Summary plot of the fiber volley amplitude ($n=7$, $p=0.91$, paired t test). Data are presented as mean \pm SEM. n.s., not significant.

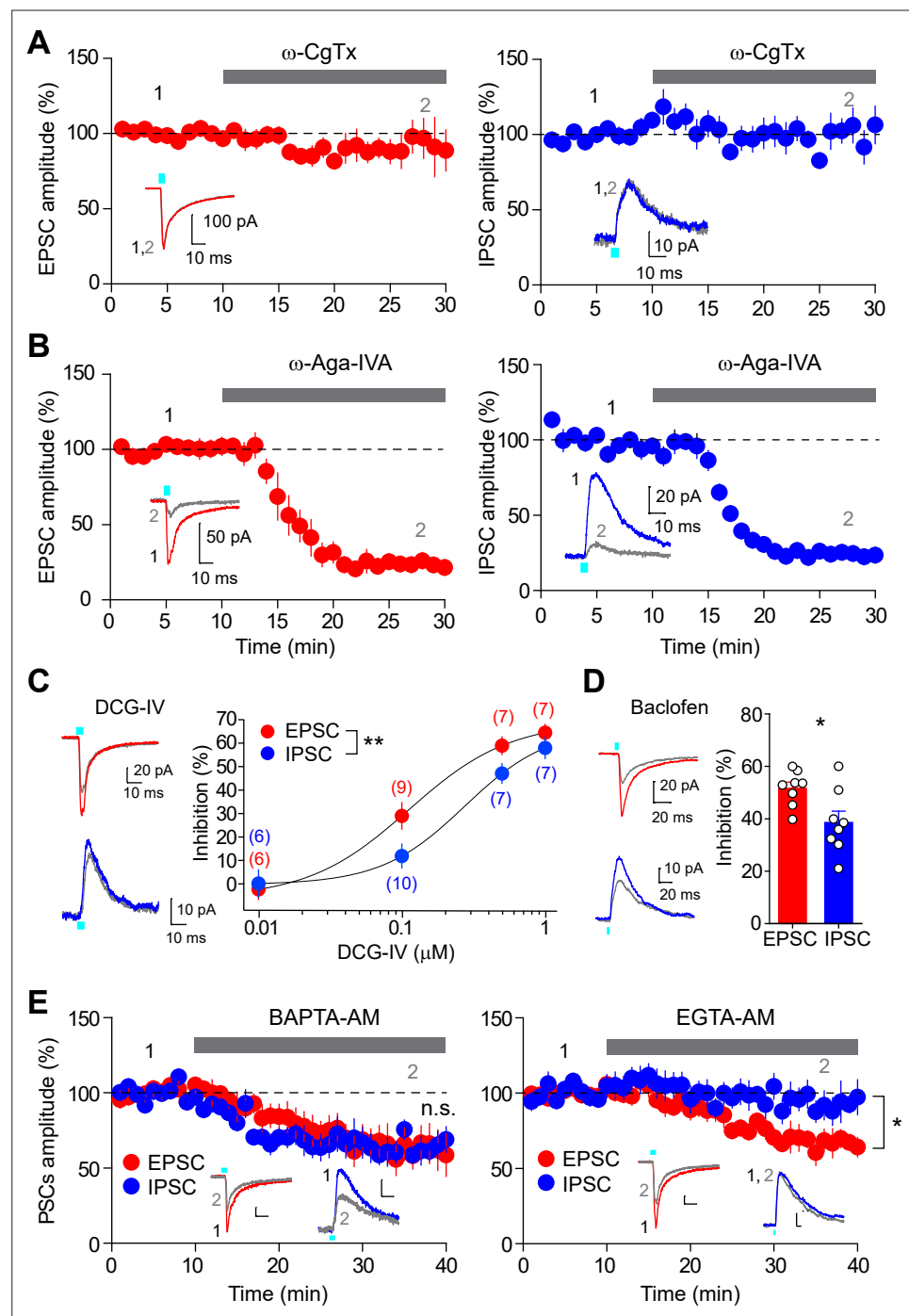


Figure 2. Different presynaptic modulation and Ca^{2+} chelator-sensitivities of glutamate/GABA co-transmission. (A) Time course summary plots showing the effects of ω -CgTx (500 nM) on co-transmission of glutamate (left) and GABA (right) at SuM-GC synapses. Insets indicate representative traces. (B) Time course summary plots showing that the co-transmission of glutamate (left) and GABA (right) at SuM-GC synapses were inhibited by ω -Aga-IVA (200 nM). Insets show representative traces. (C) (left) Representative traces before (EPSC, red; IPSC, blue) and after (gray) application of DCG-IV (0.1 μ M). (right) Summary plot of concentration-response curves. Data are fitted to the Hill equation. Numbers in parentheses indicate the number of cells. (D) (left) Representative traces before (EPSC, red; IPSC, blue) and after (gray) application of baclofen (5 μ M). (right) Summary plot of percent inhibition in the amplitudes of EPSCs and IPSCs by 5 μ M baclofen. (E) Time course summary plots showing the sensitivity of EPSCs and IPSCs to 100 μ M BAPTA-AM (left) and 100 μ M EGTA-AM (right). Insets show representative traces. Calibration: 10 pA, 10 ms. Data are presented as mean \pm SEM. * p <0.05, ** p <0.01. n.s., not significant.

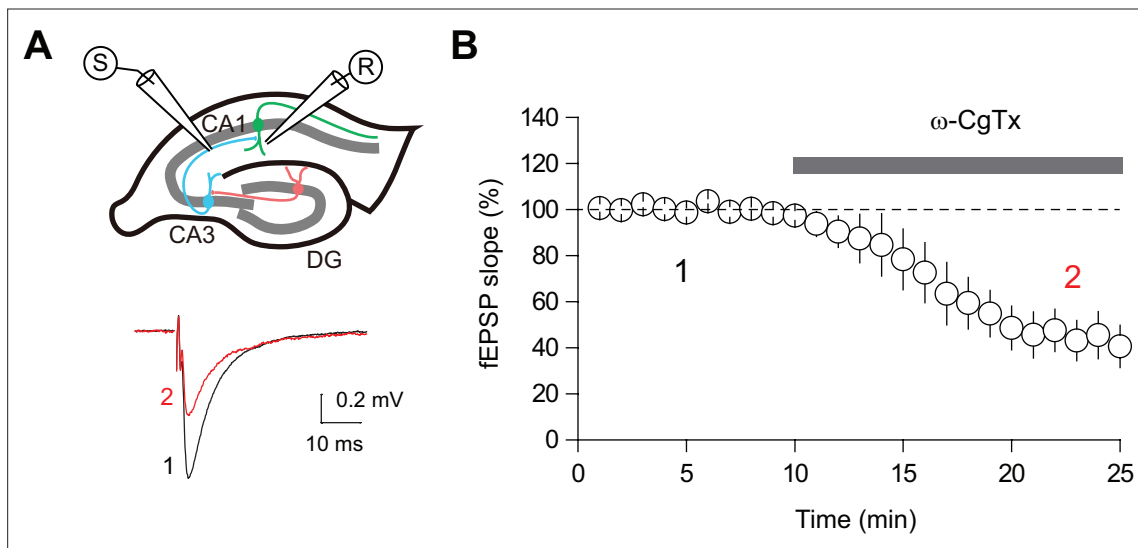


Figure 2—figure supplement 1. The effect of ω -CgTx on CA3-CA1 transmission. **(A)** (top) Schematic diagram illustrating the extracellular field excitatory postsynaptic potential recording (fEPSP) configuration. Both the recording and stimulating electrodes were placed in the stratum radiatum of CA1. (bottom) Representative fEPSP traces before (black) and after (red) application of ω -CgTx (500 nM). **(B)** Summary time course plot showing inhibition of CA3-CA1 transmission by ω -CgTx ($44.5 \pm 9.5\%$ of baseline, $n=5$, $p<0.01$, paired t-test). Data are presented as mean \pm SEM.

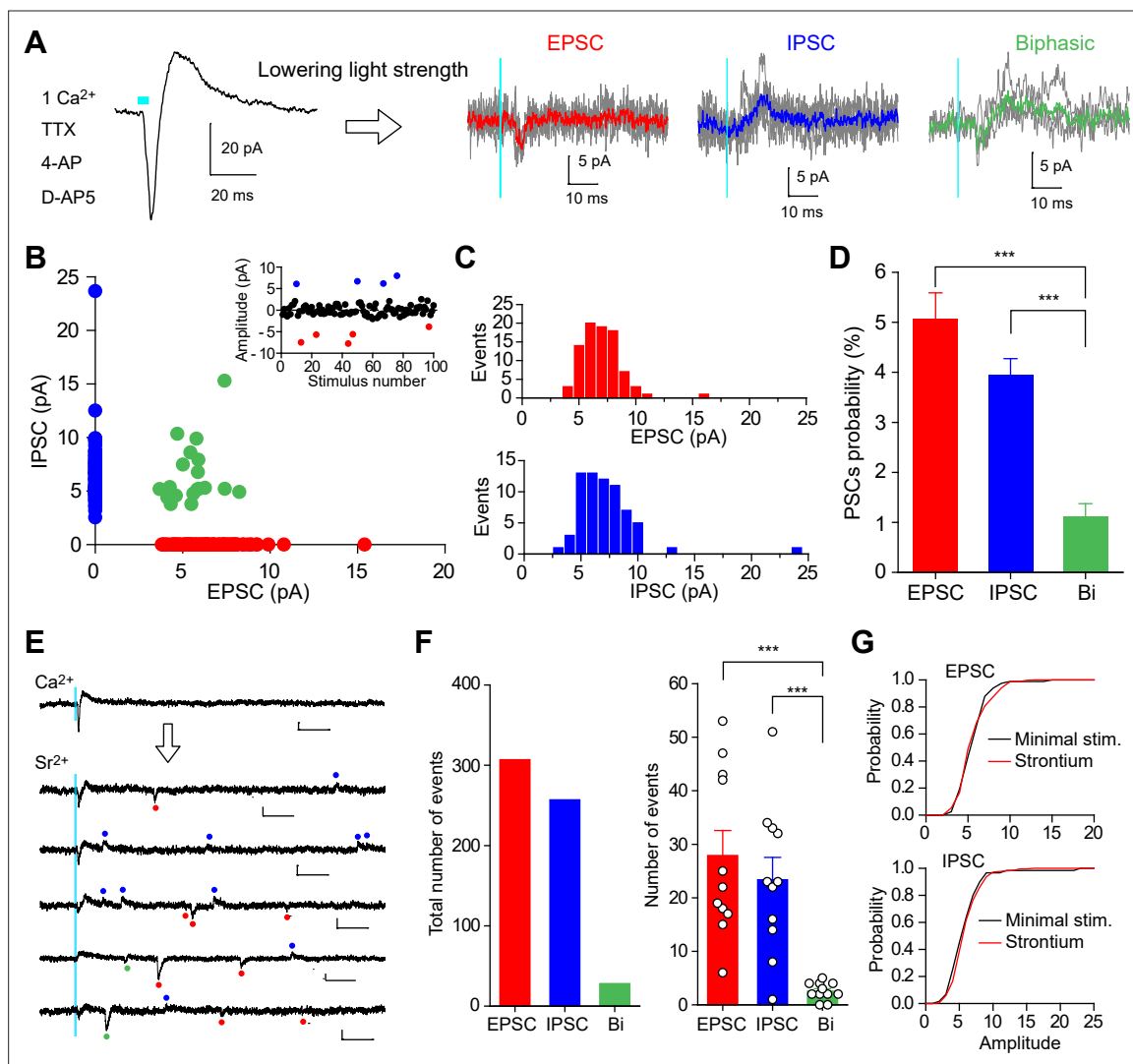


Figure 3. Uniquantal release-mediated synaptic responses evoked by minimal light stimulation or strontium-induced asynchronous release at SuM-GC synapses. **(A)** Representative traces of biphasic response elicited by light stimulation with maximum light power (left) and stochastically evoked PSCs with minimal light stimulation (100 trials for each cell) (right). Synaptic responses at SuM-GC synapses were recorded at holding potentials of -20 to -30 mV in the presence of TTX ($1 \mu\text{M}$), 4-AP (1 mM), D-AP5 ($50 \mu\text{M}$), and Ca^{2+} (1 mM). Average EPSC (red), IPSC (blue), and biphasic current (green) are superimposed on individual traces. **(B)** Scatter plot of the amplitude of IPSCs against the amplitude of EPSCs recorded from 17 cells. Success events of 172 PSCs are plotted. (Inset) A single experiment showing 100 trials with an interval of 10 sec elicited stochastically EPSCs (red) and IPSCs (blue). **(C)** Amplitude histograms of EPSCs (top) and IPSCs (bottom) in same data as in B. **(D)** Summary graph of PSCs probability. **(E)** Representative traces showing strontium-induced asynchronous release recorded from GC at holding potentials of -20 to -30 mV. The NMDA receptor antagonist D-AP5 ($50 \mu\text{M}$) was included in the extracellular solution to eliminate NMDA receptor-mediated EPSCs. Red, blue, and green points indicate detected EPSCs, IPSCs, and biphasic currents, respectively. Calibration: 10 pA , 50 ms . **(F)** (left) Summary bar graph showing the total number of asynchronous quantal responses ($n=11$, 30 trials for each cell; EPSC: 307 events; IPSC: 257 events; biphasic: 28 events). (right) Averaged number of asynchronous events showing that the majority of asynchronous events are EPSCs and IPSCs, and a few biphasic responses. **(G)** Cumulative distributions of the amplitudes of EPSCs (top) and IPSCs (bottom) for minimal light stimulation-evoked PSCs and strontium-induced PSCs (EPSC: minimal stim.: 86 events from 17 cells; strontium: 307 events from 11 cells, $p=0.72$; IPSC: minimal stim.: 67 events from 17 cells; strontium: 256 events from 11 cells, $p=0.096$, Kolmogorov-Smirnov test). Data are presented as mean \pm SEM. *** $p<0.001$.

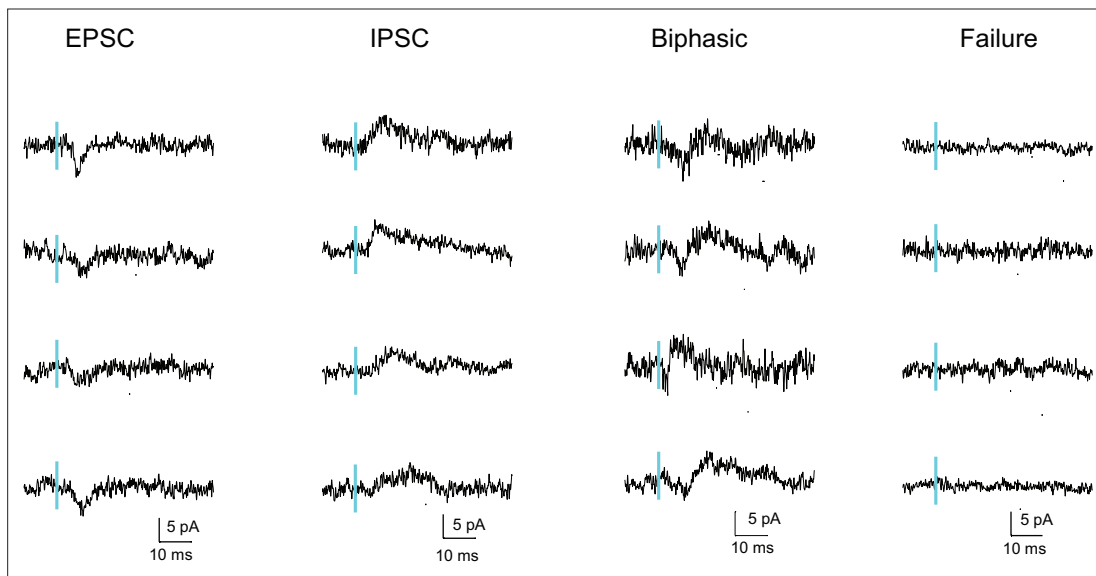


Figure 3—figure supplement 1. Minimal light stimulation-evoked synaptic responses at SuM-GC synapses. Sample traces recorded from GCs at holding potential of -20 to -30 mV in response to minimal light stimulation.

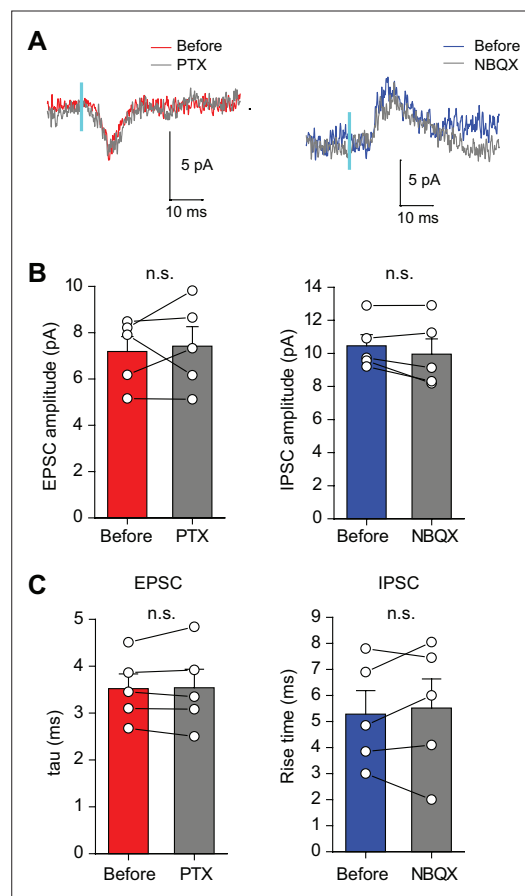


Figure 3—figure supplement 2. The amplitudes and kinetics of minimal light stimulation-evoked EPSCs or IPSCs at SuM-GC synapses were not altered by blockade of their counterpart currents. (A) Representative traces of EPSCs (left) and IPSCs (right) evoked by minimal light stimulation of SuM inputs at intermediate membrane potentials. EPSCs or IPSCs were recorded by repeating the light stimulation 100 times before, with the application of 100 μ M picrotoxin (PTX) or 10 μ M NBQX, respectively. (B) Summary plots show that the amplitudes of EPSCs and IPSCs were not changed after application of PTX or NBQX, respectively (EPSC: before: 7.2 ± 0.6 pA; PTX: 7.4 ± 0.8 pA, $n=5$, $p=0.71$, paired t test; IPSC: before: 10.5 ± 0.7 pA; NBQX: 10.0 ± 0.9 pA, $n=5$, $p=0.18$, paired t test). (C) Summary plots of the decay time constant of EPSCs (tau, single-exponential fit) and rise time of IPSCs (10%–90% of IPSC peak amplitude; tau: before: 3.5 ± 0.3 ms; PTX: 3.5 ± 0.4 ms, $n=5$, $p=0.84$, paired t test; rise time: before: 5.3 ± 0.9 ms; NBQX: 5.5 ± 1.1 ms, $n=5$, $p=0.60$, paired t test). Data are presented as mean \pm SEM. n.s., not significant.

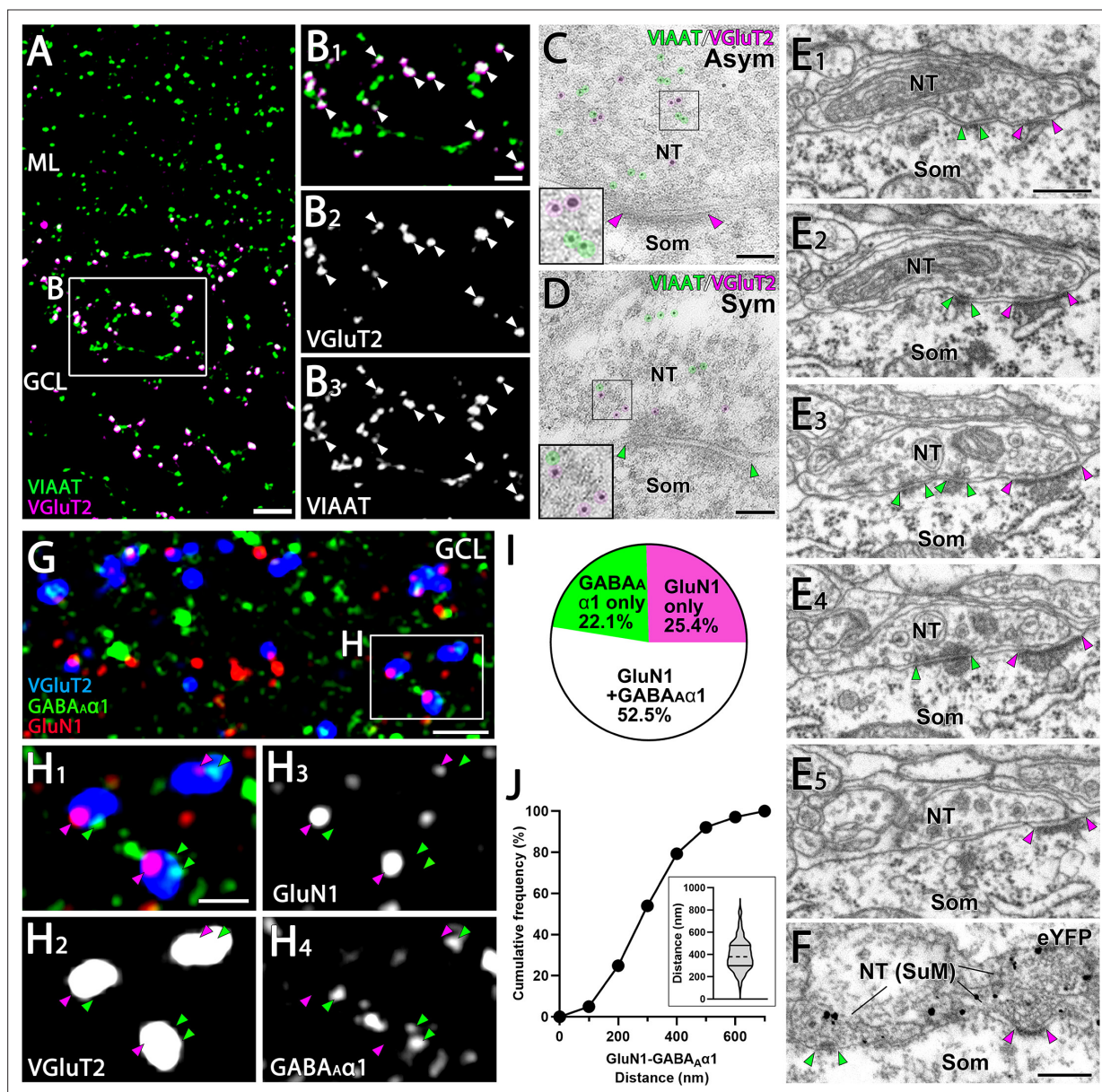


Figure 4. Close association of GluN1 and GABA α 1 facing the identical SuM terminals. (A, B) Double immunofluorescence for VIAAT (green) and VGLUT2 (magenta) in the GC layer of the DG. (B) Higher magnification images of the boxed area in (A) show that VGLUT2-positive terminals are consistently co-labeled with VIAAT (white arrowheads). (C, D) Post-embedding immunogold EM shows immunogold particles for VIAAT (green, 5 nm) and VGLUT2 (magenta, 10 nm) colocalizing within the same terminal, forming asymmetric (C) and symmetric (D) synapses. NT, nerve terminal; Som, soma. (E) Five consecutive EM images depict a single NT forming both asymmetric and symmetric synapses with a GC soma. The postsynaptic densities of the asymmetric and symmetric synapses are indicated by magenta and green arrowheads, respectively. (F) A pre-embedding immunogold EM image demonstrates a single NT from SuM, labeled with eYFP, forming both asymmetric and symmetric synapses with a GC soma. The postsynaptic densities are similarly marked by magenta and green arrowheads. (G, H) Triple immunofluorescence for GluN1 (red), GABA α 1 (green), and VGLUT2 (blue) in the GC layer of the DG. (H) Higher magnification of the boxed region in (G). Magenta arrowheads indicate GluN1 and green arrowheads indicate GABA α 1, both apposed to VGLUT2 puncta. (I) The proportion of VGLUT2-positive terminals in the GC layer associated with GluN1 and/or GABA α 1 immunoreactivity. Data are based on measurements from 634 VGLUT2-positive terminals from two mice. (J) Cumulative distribution of the distance between GluN1 and GABA α 1 puncta associated with VGLUT2-positive terminals in the GC layer that are double-labeled for GluN1 and GABA α 1. Data are based on measurements from 241 VGLUT2-positive terminals from two mice (violin plot shown in the inset). The dashed line within each violin plot represents the median, while the solid lines at the top and bottom indicate the 75th and 25th percentiles, respectively. Scale bars: A, 5 μ m; B, 2 μ m; C, D, 100 nm; E, F, 400 nm; G, 5 μ m; H, 1 μ m.

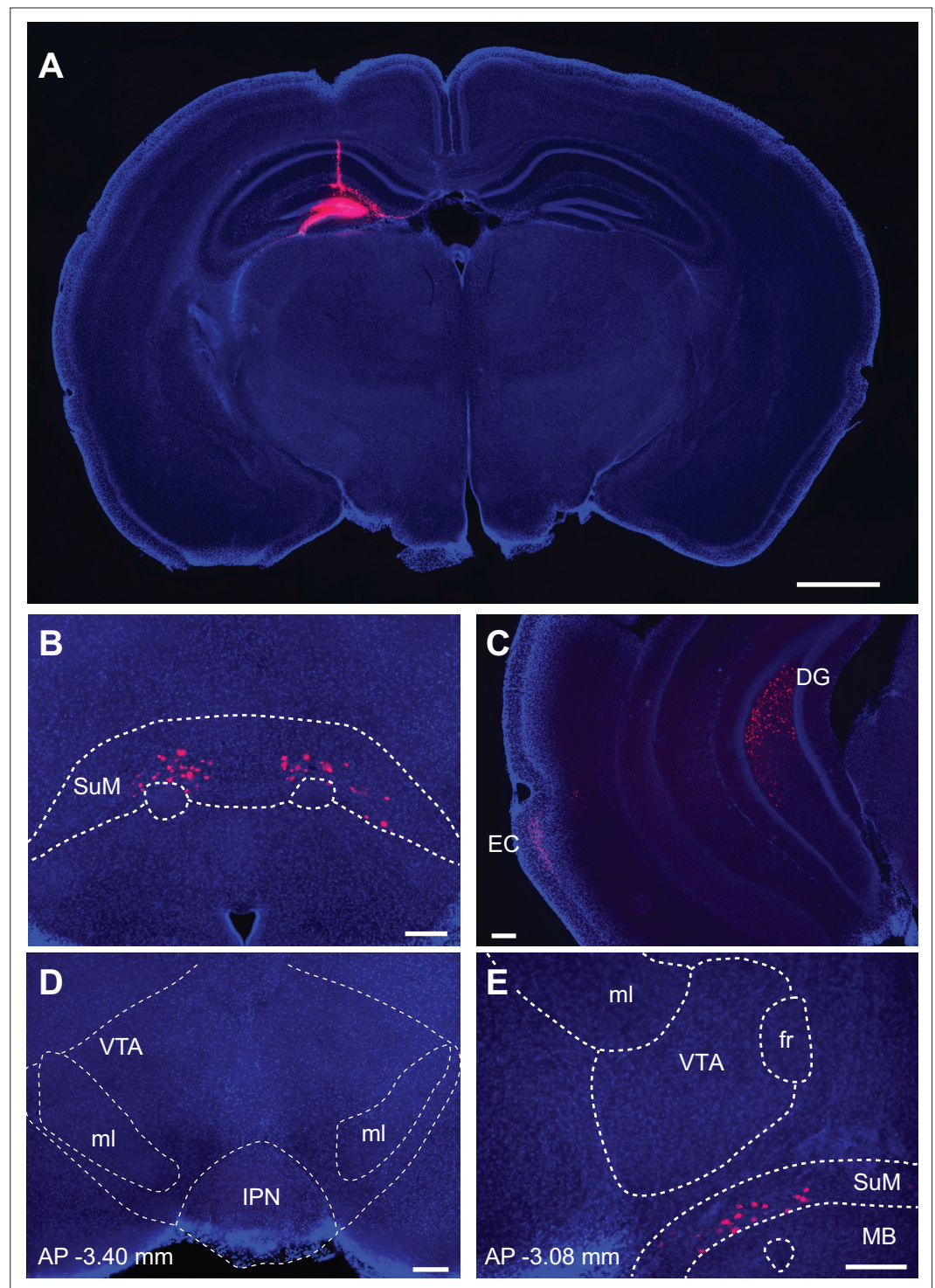


Figure 4—figure supplement 1. DG receives monosynaptic input from SuM and EC, but not from VTA. (A) Unilateral injection of retrograde tracers (fluorescent microspheres; red) into the dorsal DG. Fluorescence image of a coronal brain slice at the injection site. (B) Retrogradely labeled neurons were observed in the ipsilateral and contralateral SuM. (C) Ipsilateral EC cells were retrogradely labelled. (D, E) Retrograde labelling was not observed in the VTA at two different positions (−3.40 mm and −3.08 mm posterior to bregma; *Paxinos and Franklin, 2001*). ml, medial lemniscus; IPN, interpeduncular nucleus; fr, fasciculus retroflexus; MB, mammillary bodies. Scale bars: A, 1 mm; B–E, 200 μ m.

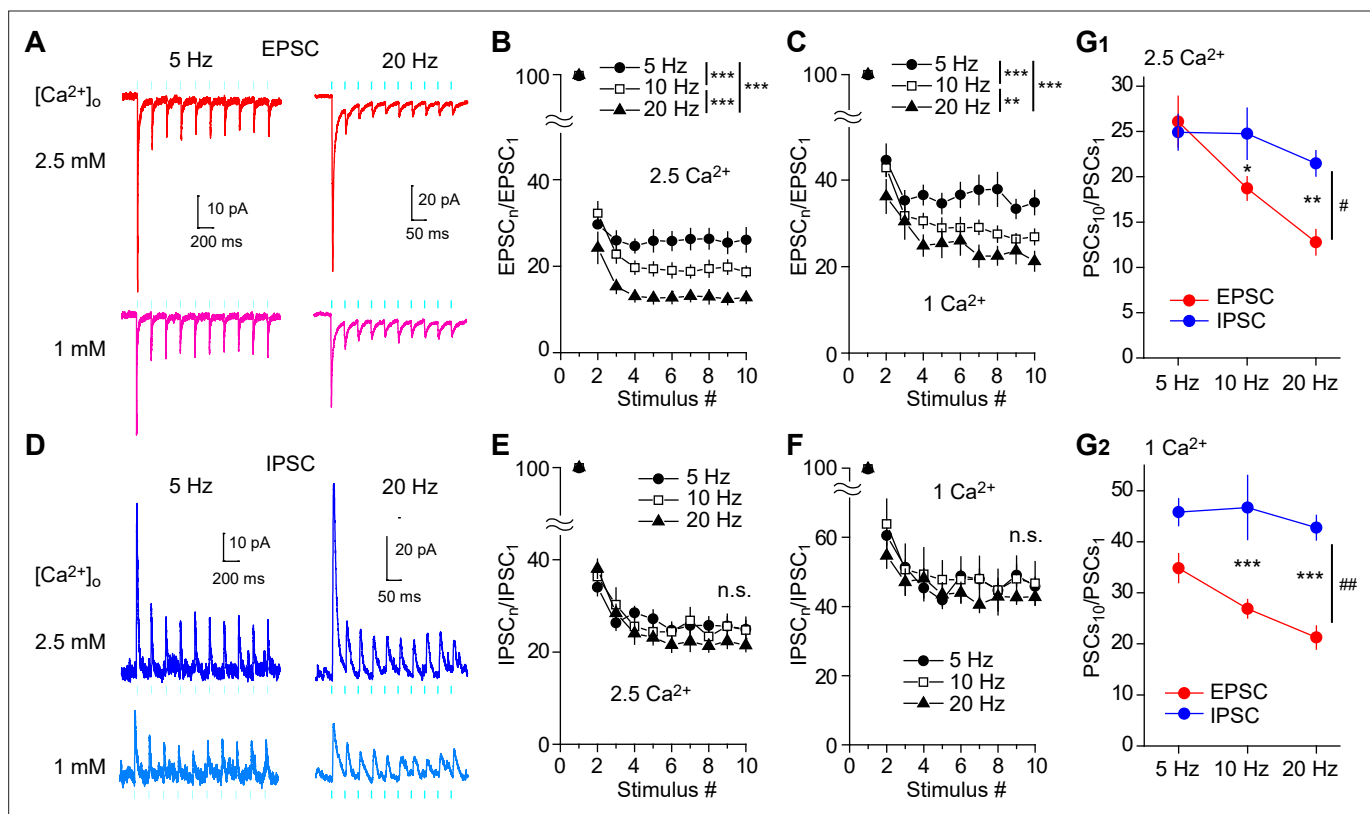


Figure 5. Frequency-dependent shift of glutamate/GABA co-transmission balance of SuM inputs in GCs. **(A, D)** Representative traces of EPSCs ($V_h = -70$ mV) **(A)** and IPSCs ($V_h = 0$ mV) **(D)** in response to 10 light stimuli at 5 Hz (left) or 20 Hz (right) in 2.5 mM (top) or 1 mM (bottom) extracellular Ca^{2+} . **(B)** Summary graph of normalized EPSC amplitude plotted against the stimulus number in 2.5 mM extracellular Ca^{2+} . Two-way repeated measures ANOVA, $F_{(2,16)} = 13.0$, $p < 0.001$, $n = 9$ or 10 ; Tukey post hoc test: $***p < 0.001$. **(C)** Same as **(B)**, but recorded in 1 mM extracellular Ca^{2+} . Two-way repeated measures ANOVA, $F_{(2,16)} = 11.4$, $p < 0.001$, $n = 9$ or 10 ; Tukey post hoc test: $**p < 0.01$, $***p < 0.001$. **(E)** Summary graph of normalized IPSC amplitude plotted against stimulus number in 2.5 mM extracellular Ca^{2+} . Two-way repeated measures ANOVA, $F_{(2,16)} = 0.003$, $p = 0.997$, $n = 9$. **(F)** Same as **(E)**, but recorded in 1 mM extracellular Ca^{2+} . Two-way repeated measures ANOVA, $F_{(2,16)} = 0.02$, $p = 0.981$, $n = 9$. **(G)** Summary plots showing the normalized amplitudes of 10th EPSCs and IPSCs at 5 Hz, 10 Hz, and 20 Hz in 2.5 mM extracellular Ca^{2+} (G1: two-way repeated measures ANOVA, $F_{(1,7)} = 8.03$, $^{\#}p < 0.05$, $n = 9$ or 10 ; Tukey's post hoc test, EPSC versus IPSC, $*p < 0.05$, $**p < 0.01$), or in 1 mM extracellular Ca^{2+} (G2: two-way repeated measures ANOVA, $F_{(1,7)} = 21.76$, $^{\#}p < 0.01$, $n = 9$ or 10 ; Tukey's post hoc test, EPSC versus IPSC, $***p < 0.001$). n.s., not significant. Data are presented as mean \pm SEM.

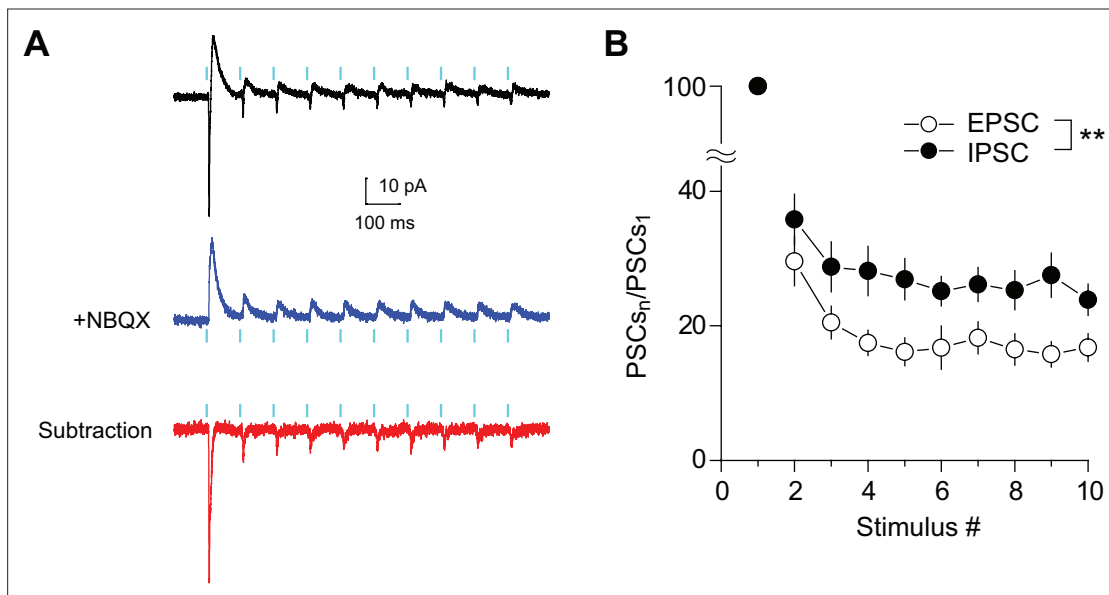


Figure 5—figure supplement 1. Short-term changes in EPSC/IPSC ratio during train stimulation at SuM-GC synapses. **(A)** Representative PSCs in response to 10 light pulses at 10 Hz recorded from GC at holding potentials of -30 mV before (black) and after application of $10 \mu\text{M}$ NBQX (blue). The EPSC (red) was isolated by subtracting the blue trace from the black trace. $1 \mu\text{M}$ TTX, $500 \mu\text{M}$ 4-AP, $50 \mu\text{M}$ D-AP5, $100 \mu\text{M}$ LY341495, and $3 \mu\text{M}$ CGP55845 were included in the extracellular solution throughout the experiments. **(B)** Summary graph of normalized EPSC and IPSC amplitudes plotted against stimulus number. Two-way repeated measures ANOVA, $F_{(1,7)} = 17.5$, $p < 0.01$, $n = 8$. Data are presented as mean \pm SEM. $**p < 0.01$.

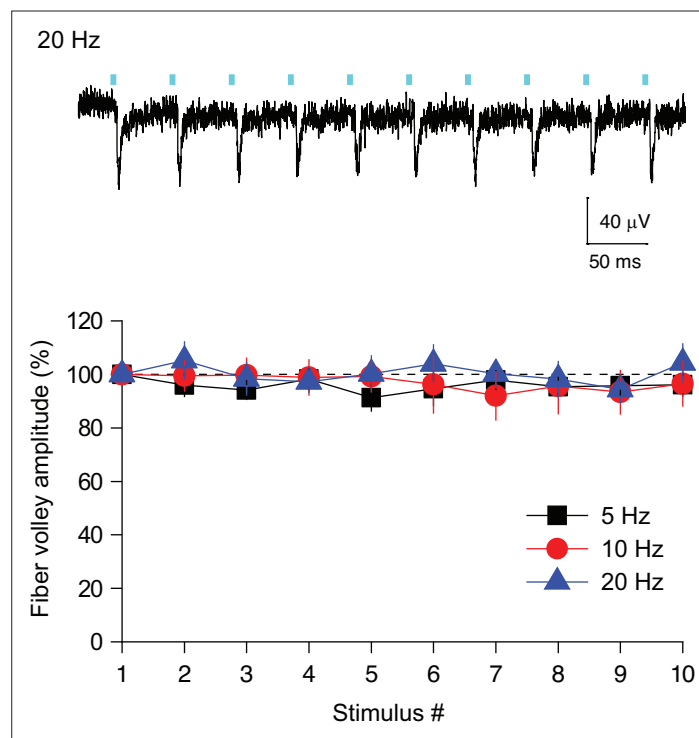


Figure 5—figure supplement 2. High fidelity activation of ChR2-expressing SuM fibers during trains. (top) Representative trace of the extracellularly recorded fiber volley from supragranular layer in response to 10 light stimuli at 20 Hz. (bottom) Summary graph of normalized fiber volley amplitude plotted against the stimulus number. 5 Hz: One-way ANOVA, $F_{(9,40)} = 0.41$, $p=0.92$, $n=5$. 10 Hz: One-way ANOVA, $F_{(9,50)} = 0.14$, $p=0.99$, $n=6$. 20 Hz: One-way ANOVA, $F_{(9,50)} = 0.35$, $p=0.95$, $n=6$. Data are presented as mean \pm SEM.

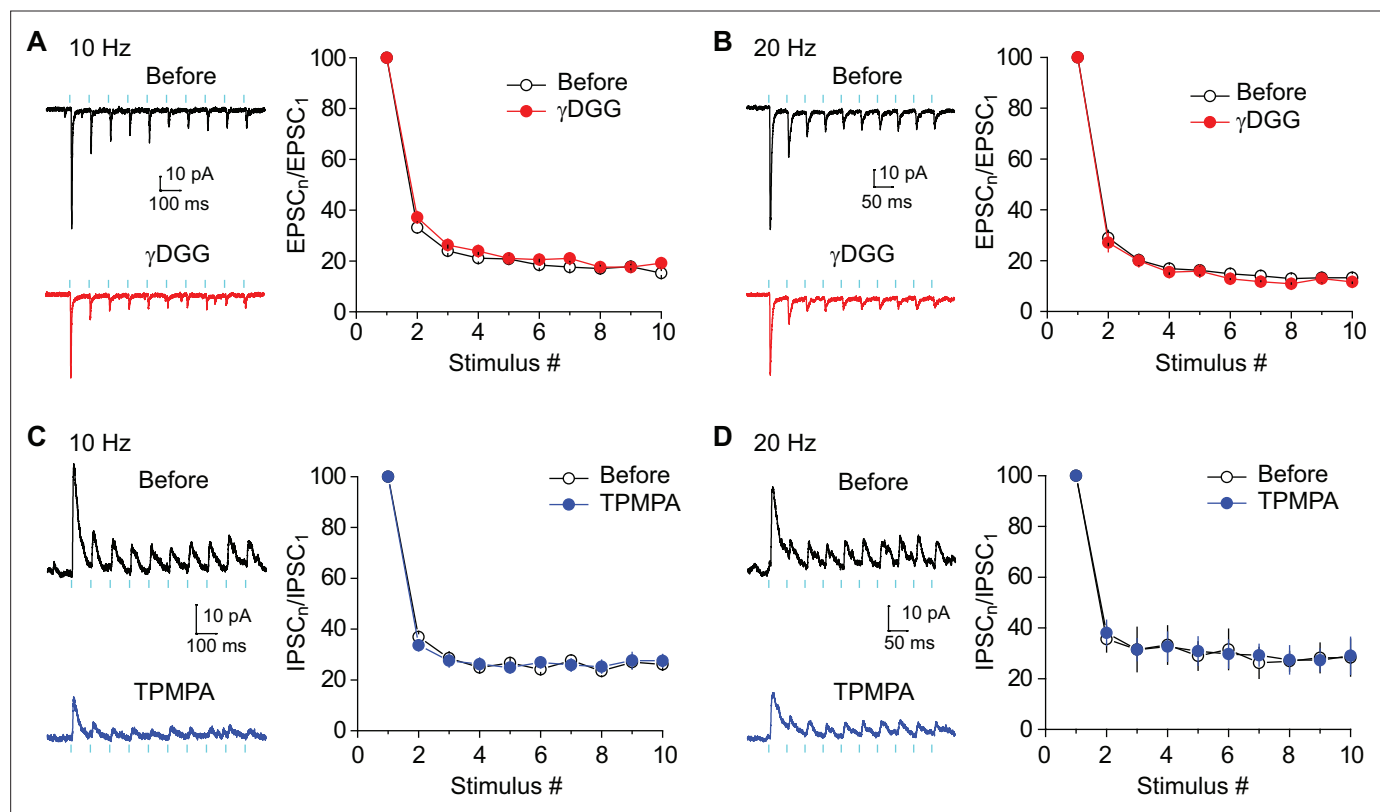


Figure 5—figure supplement 3. Preventing postsynaptic saturation and desensitization does not alter short-term depression of EPSCs and IPSCs. **(A and B)** (left) Representative traces showing EPSCs in response to 10 Hz **(A)** or 20 Hz **(B)** light stimulation before (top) and after (bottom) application of 2 mM γ DGG. (right) Summary graph of normalized EPSC amplitudes plotted against stimulus number. 10 Hz: Two-way repeated measures ANOVA, $F_{(1,7)} = 1.78$, $p=0.22$, $n=8$. 20 Hz: Two-way repeated measures ANOVA, $F_{(1,7)} = 0.65$, $p=0.45$, $n=8$. **(C and D)** (left) Representative traces showing IPSCs in response to 10 Hz **(C)** or 20 Hz **(D)** light stimulation before (top) and after (bottom) application of 300 μ M TPMPA. (right) Summary graph of normalized IPSC amplitudes plotted against stimulus number. 10 Hz: Two-way repeated measures ANOVA, $F_{(1,5)} = 1.02$, $p=0.44$, $n=6$. 20 Hz: Two-way repeated measures ANOVA, $F_{(1,4)} = 0.21$, $p=0.67$, $n=5$. Data are presented as mean \pm SEM.

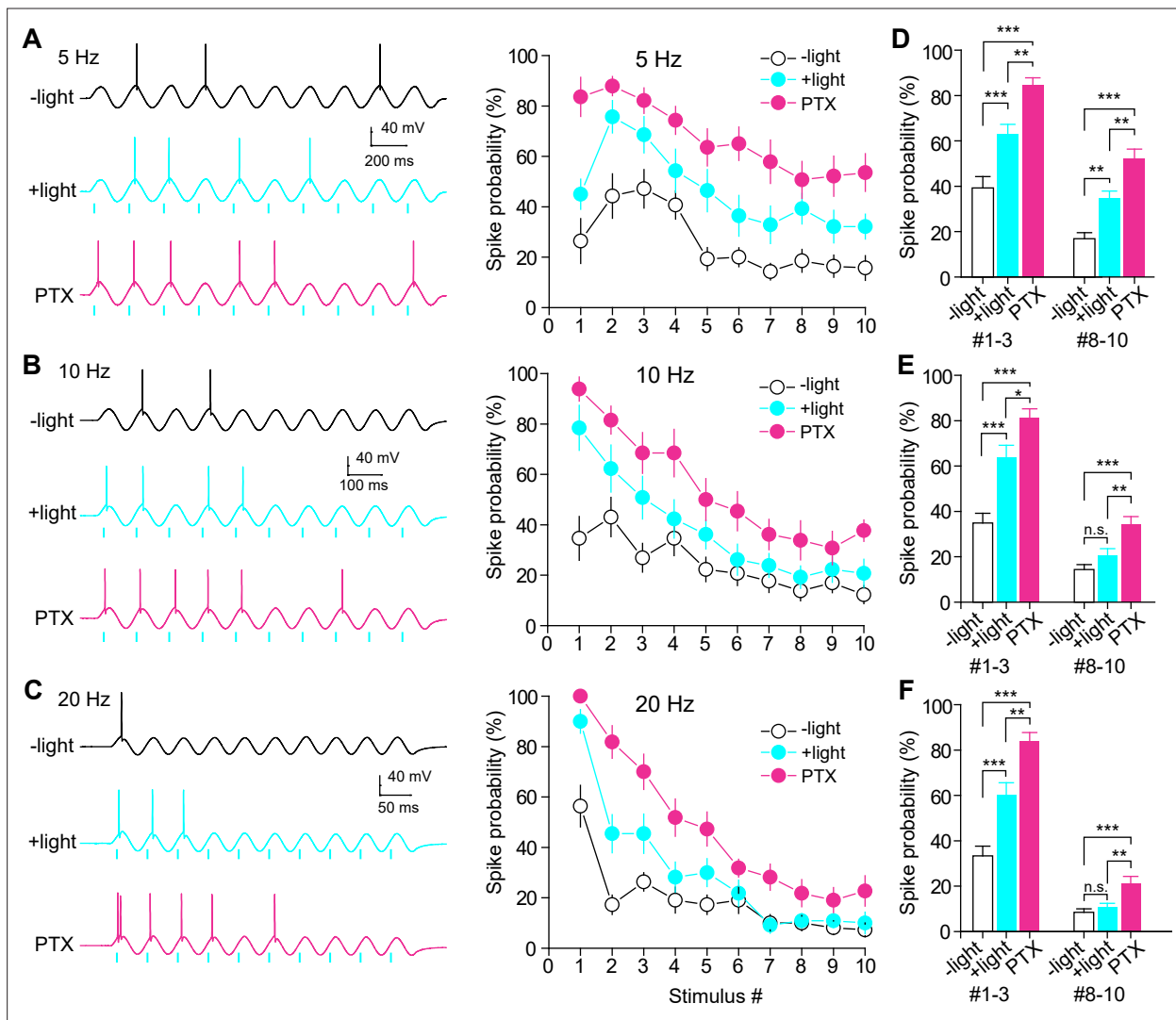


Figure 6. Frequency-dependent modulation of GC firing by SuM inputs. **(A–C)** (left) Representative traces showing GC spikes in response to sinusoidal current injections without (top) and with (middle) paired light stimulation of SuM inputs at 5 Hz **(A)**, 10 Hz **(B)**, and 20 Hz **(C)**. Bottom trace showing the GC response to sinusoidal current injection paired with light stimulation in the presence of 100 μ M picrotoxin (PTX). (right) Summary graph of spike probability against stimulus number. **(D–F)** Summary plots of spike probability at initial and last three stimulus numbers at 5 Hz **(D)**, 10 Hz **(E)**, and 20 Hz **(F)**. The spike probabilities of stimulus numbers 1–3 and 8–10 were averaged. **(D)** one-way ANOVA, $n=14$, $F_{(2,123)} = 28.8$, $p<0.001$ (#1–3), $F_{(2,123)} = 25.8$, $p<0.001$ (#8–10); Tukey's post hoc test, $***p<0.001$, $**p<0.01$. **(E)** one-way ANOVA, $n=13$, $F_{(2,114)} = 26.3$, $p<0.001$ (#1–3), $F_{(2,114)} = 11.8$, $p<0.001$ (#8–10); Tukey's post hoc test, $***p<0.001$, $**p<0.01$, $*p<0.05$, n.s., not significant. **(F)** one-way ANOVA, $n=11$, $F_{(2,96)} = 31.4$, $p<0.001$ (#1–3), $F_{(2,96)} = 9.2$, $p<0.001$ (#8–10); Tukey's post hoc test, $***p<0.001$, $**p<0.01$, n.s., not significant. Data are presented as mean \pm SEM.

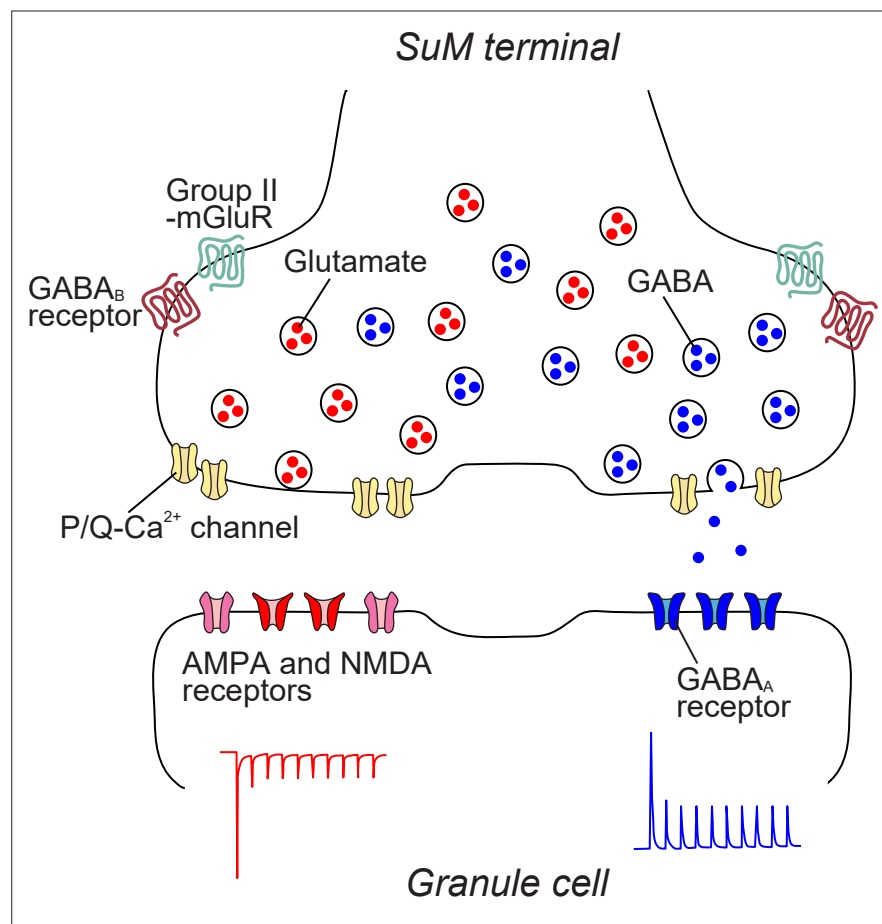


Figure 7. Working hypothesis of synaptic architecture of SuM-GC synapse. A single SuM terminal contains distinct glutamatergic and GABAergic vesicles, which are regulated by P/Q-type Ca^{2+} channels and also modulated by group II mGluRs and GABA_B receptors. Glutamatergic and GABAergic vesicles are loosely and tightly coupled with Ca^{2+} channels, respectively. At the postsynaptic site of GCs, AMPA/NMDA and GABA_A receptors are distributed separately. Based on their molecular composition, glutamatergic and GABAergic synapses are established independently, achieving the distinct glutamatergic and GABAergic transmission.